Digest Journal of Nanomaterials and Biostructures Vol. 8, No. 1, January - March 2013, p. 263 - 272

STRUCTURAL, MORPHOLOGICAL, OPTICAL AND THERMAL PROPERTIES OF THE $ZnTa_2O_6$ NANOMATERIALS OBTAINED BY SOLID - STATE METHOD

M. BÎRDEANU, A.–V. BÎRDEANU[a], E. FAGADAR-COSMA[b], C. ENACHE[b], I.MIRON, I.GROZESCU[*]

National Institute for Research and Development in Electrochemistry and Condensed Matter, 1 Plautius Andronescu Street, 300224 Timisoara, Romania

[a]*National R&D Institute for Welding and Material Testing - ISIM Timişoara, 20 M. Viteazu Ave., 300222, Timisoara, Romania*

[b]*Institute of Chemistry Timisoara of Romanian Academy, 24 M. Viteazu Ave, 300223-Timisoara, Romania*

Nanocrystalline $ZnTa_2O_6$ has been synthesized using tantalum (V) oxide and zinc nitrate by solid-state method. The crystal structure and microstructure, phase composition and the absorption of $ZnTa_2O_6$ powders were characterized by X-ray diffraction, FT/IR measurements, UV-VIS measurements, SEM and AFM techniques. Physico-chemical transformations during thermal treatment were performed by thermal analysis (DTA/DTG/TG). The effects of pH values on the crystal structure and microstructure of $ZnTa_2O_6$ nanopowders were also investigated. XRD results show that the single phase of $ZnTa_2O_6$ for synthesized powder can be obtained by heating the nanomaterials at 1100 °C for three hours soaking time. The average particle size of $ZnTa_2O_6$ is almost tailored, having the mean values of 35 nm, 38 nm and 43 nm respectively, with varying the pH conditions from acid to basic ones. This narrow nanometer size was also confirmed by AFM measurements. DTG/DTA/TG results show a main significant feature, independent of the pH value, taking place around 850 °C.

(Received November 11, 2012; Accepted January 25, 2013)

Keywords: nanomaterials; $ZnTa_2O_6$, solid-state method; X-ray spectra

1. Introduction

Developments of nanotechnology attract nowadays substantial interest because nanomaterials exhibit unique optical [1-4], electrical [5] thermal [6] and catalytic properties [7].

The recent approaches concerning photocatalytic activity under visible-light irradiation were focused on substitution of Zn^{2+} in the lattice of ZnO by Ta^{5+}. Experimental reports [8] demonstrated that the additions of the Ta as dopant are increasing the lattice constants and bandgap of the nanocrystals and supplementary improves the photocatalytic activity.

Nanocrystalline $ZnTa_2O_6$ with different crystal structures, as a member of tantalite's, is expected to act as a promising photocatalyst. Literature data already offered examples about $ZnTa_2O_6$ samples, which showed excellent performances in the photodegradation of methyl orange under UV light irradiation with the band gap of about 4.35 eV [9].

Nanocrystalline $ZnTa_2O_6$ were found to be promising candidates for application in microwave devices [10 - 12] and show excellent performances in environment and energy fields [8]. Methods for preparation of nanocrystalline $ZnTa_2O_6$ are usually wet chemical methods, including sol–gel, solid-state method, etc. [8 - 10, 12 - 15].

[*]Corresponding author: ioangrozescu@gmail.com

$ZnTa_2O_6$ nanopowders were synthesized using $Zn(NO_3)_2$ and Ta_2O_5 as the starting materials by solid-state method.

2. Experimental procedure

The $ZnTa_2O_6$ nanocrystals were obtained by solid-state method. The starting materials used during the synthesis were: tantalum(V) oxide - Ta_2O_5 (99.99%, Merck) and zinc nitrate – $Zn(NO_3)_2$ x $6H_2O$ (99.99%, Merck) while keeping the molar ratio at 1:1. A suspension was obtained using the calculated amounts of the starting materials and double distilled water which was homogenized by a magnetic stirrer for 6h at 90ºC. The pH of the obtained mixture was adjusted by using a 10M concentration sodium hydroxide (NaOH) solution. The pH values used for the synthesis were fixed at: 12.5, 10.5 and 7. The resulting product was filtered, five times washed using distilled water and three times more by using ethanol and finally dried in air for 24 h at room temperature. All the obtained mixtures were afterwards heated at 1000 ºC and 1100 ºC for 3 h soaking time. The heating and cooling rate of the heated furnace was set at 5ºC/min. The phase identification of the synthesized powders was investigated by X-ray diffraction (XRD) on an X'pert Pro MPD X-ray diffractometer, with monochromatic Cu Kα (λ = 1.5418 Å) incident radiation, and FT/IR measurements on a JASCO 430 FT-IR spectrometer, in the 4000-400 cm^{-1} spectral range, using KBr pellets technique. For each obtained ZnTa2O6 nanomaterials the elementary cell volume and parameters were calculated.

For the morphology and dimension of the sample particles, field emission-scanning electron microscopy – SEM / EDAX (Model INSPECT S), and atomic force microscopy – AFM (Model Nanosurf® EasyScan 2 Advanced Research) were used. The band gap of the $ZnTa_2O_6$ nanocrystals was calculated by recording the diffuse reflectance spectrum at room temperature using UV-VIS-NIR spectrometer Lambda 950.

The decomposition and crystallization behavior of the samples were analyzed by thermogravimetry and differential thermal analysis with a TGA / SDTA 851-LF Mettler-Toledo apparatus, in air atmosphere, in the 25–1000 °C temperature range at a heating rate of 20 °C/min.

3. Results and discussions

Fig. 1 shows the XRD patterns of the $ZnTa_2O_6$ nanomaterials (a) un- heated pH=12.5; (b) un- heated pH=10.5; (c) un- heated pH=7; (d) heated for 3 h at 1000 °C pH=12.5; (e) heated for 3 h at 1000 °C pH=10.5; (f) heated for 3 h at 1000 °C pH=7; (g) heated for 3 h at 1100 °C pH=12.5; (h) heated for 3 h at 1100 °C pH=10.5; (k) heated for 3h at 1100 °C pH=7. One can observe from the a), b) and c) spectra from Fig. 1 that three material phases do appear, i.e. the phase of the Ta_2O_5 starting materials, but also, the formation $ZnTa_2O_6$ phase. For the samples calcined at 1000 °C for 3h soaking time (Fig. 1 d, e, f) one can observe that the Ta_2O_5 specific peaks intensities are diminished in comparison with those calcined at lower temperatures, the diffraction maxima corresponding to $Zn(NO_3)_2$ phase disappear, and more diffraction maxima, corresponding to $ZnTa_2O_6$ crystalline phase, appear.

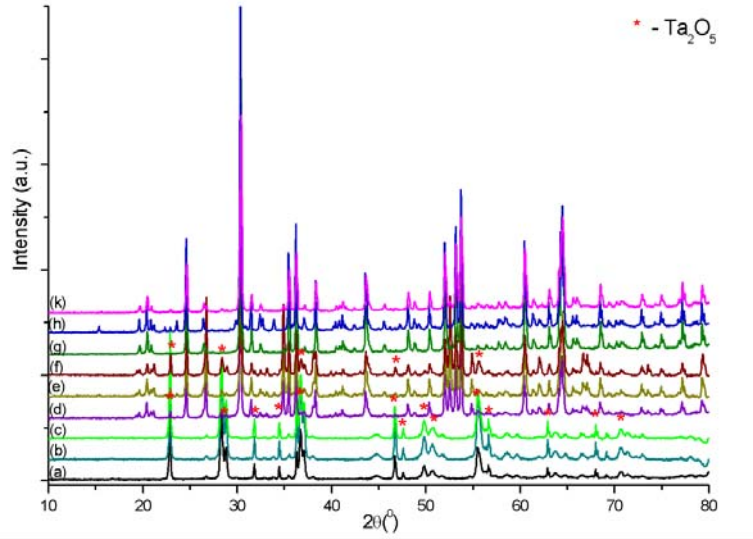

Fig.1 The XRD patterns of $ZnTa_2O_6$: (a) un- heated pH=12.5: (b) un- heated pH=10.5, (c) un- heated pH=7; (d) heated 1000 °C pH=12.5; (e) heated 1000 °C pH=10.5; (f) heated 1000 °C pH=7; (g) heated 1100 °C pH=12.5; (h) heated 1100 °C pH=10.5; (k) heated 1100 °C pH=7

The XRD spectra of samples thermally treated at 1100 °C, show the main diffraction maxima of $ZnTa_2O_6$ crystalline phase (Fig 1. g, h si k), which are in good agreement with JCPDS #76-1826, belonging to the space group *Pbcn (60)*. The intensity of the peaks relative to the background signal demonstrates high purity and good quality of the samples. All the specimens showed to 2θ=30.276°, (131) peak with highest intensity in the XRD patterns.

The elementary cell volume and parameters of $ZnTa_2O_6$ samples were calculated and are presented in Table 1.

Table 1 The elementary cell characteristics.

Material: $ZnTa_2O_6$ heated at 1100 °C for 3 h	**Elementary cell parameters (Å)**			**Angle (°)**			**Elementary cell's volume ($V/10^6/pm^3$)**
	a	b	c	α	β	υ	
pH=12.5	4.692	17.027	5.052	90	90	90	403.565
pH=10.5	4.686	17.092	5.071	90	90	90	406.167
pH=7	4.693	17.061	5.064	90	90	90	405432

The mean crystallite size (d) of the powder samples was calculated using Scherrer's formula (1) [16]:

$$d = \frac{K\lambda}{\left(\beta^2 - \beta_0^2\right)^{1/2}\cos\theta} \quad (1)$$

where β is the half-width of the diffraction peak in radians, β_0 corresponds to the instrumental broadening, K = 180/π, λ is the X-ray wavelength, and θ is the Bragg diffraction angle. The average crystallite size determined from XRD line broadening for the samples of $ZnTa_2O_6$ thermally treated at 1100 ºC was: 35 nm (pH=12.5), 43 nm (pH=10.5) and 38 nm (pH=7), respectivelly.

In order to determine the existence of non-crystalline phases, which could be present in mixture with crystalline phases, FT-IR spectroscopy measurements were done beside the X-ray diffraction analysis.

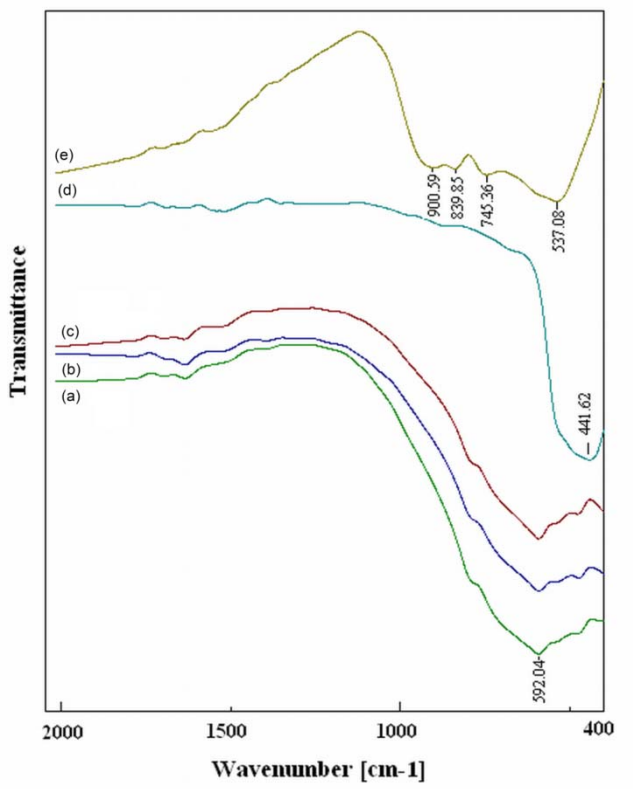

Fig.2. FT/IR spectra of the obtained $ZnTa_2O_6$: (a) pH=12.5; (b) pH=10.5; (c) pH=7; (d) $Zn(NO_3)_2$; (e) Ta_2O_5

Fig. 2 a, b and c presents the FT/IR spectra of the obtained $ZnTa_2O_6$ nanomaterials at different values of the pH and also, the Fig.2 additionally present the FT/IR spectra of the $Zn(NO_3)_2$ and Ta_2O_5 precursors for comparison. The obtained spectra were done by transmittance in the range of 2000-400cm^{-1}. The spectrum of Ta_2O_5 sample showed a broad and intensive IR band resulted by overlapping of four next located bands at 900.59 cm^{-1}, 839.85 cm^{-1}, 745.37 cm^{-1} and 537.08 cm^{-1}, whereas $Zn(NO_3)_2$ sample showed only one intense band at 441.62 cm^{-1}.

Due to the fact that the charge of Ta^{5+} is larger than that of Zn^{2+}, the force constant associated with Ta-O vibration is larger in comparison with the vibrations involving Zn-O ions.

Although, the frequency of Ta-O appears at higher values compared to that of Zn-O vibration [17].

On the other hand, the M-O distance is generally not depending on the coordination number or the oxidation state of the metal [18]. In Fig. 2 a, b and c which correspond to samples $ZnTa_2O_6$, a new band, located at 592.04 cm^{-1}, distinct from specific Ta-O and Zn-O FT-IR bands can be noticed. This new appearing band can be assumed that belongs to Zn-O-Ta bond [8], especially because Zn–O bond is not as strong as the Ta–O bond, so that the intermediate position can be an agreed explanation.

Figs. 3 a, b and c present the morphology of the $ZnTa_2O_6$ nanoparticles obtained by using different values of the solution's pH and the formation of agglomerates and their disposition in "chains", can be noticed. The chain distribution of the obtained $ZnTa_2O_6$ nanoparticles is more significant for pH=7 (Fig. 3 c), while the particles are more uniform compared to the ones obtained at pH=12.5 and pH=10.5.

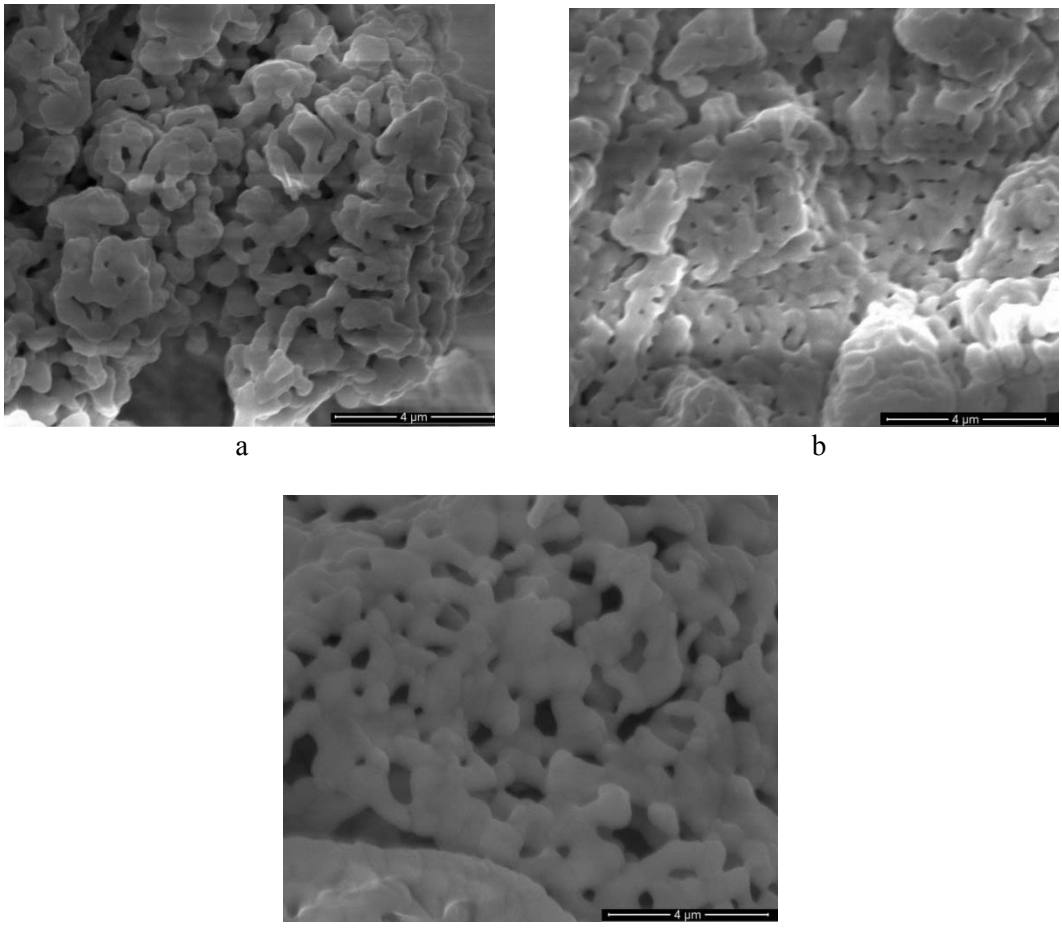

a b

c

Fig. 3 The SEM of $ZnTa_2O_6$ powders obtained with different pH values heated at 1100°C. (a) pH=12.5, (b) pH= 10.5, (c) pH= 7

Figs. 4 a, b and c shows the AFM images of surface morphology for the heated $ZnTa_2O_6$ at 1100 °C for 3 h: a) pH=12.5, b) pH= 10.5 and c) pH= 7, scan size is 1µm x 1µm. The samples were measured with the use of non-contact mode cantilever, vibrating with small amplitude, experiencing a non-uniform force field near the sample surface. Therefore this method provides measurement of Van der Waals, electrostatic, magnetic forces near the surface. Interaction force can be very small (about 10^{-12} N) that allows investigation of very sensitive objects or those intimate coupled to a substrate surface, without any destruction or displacement.

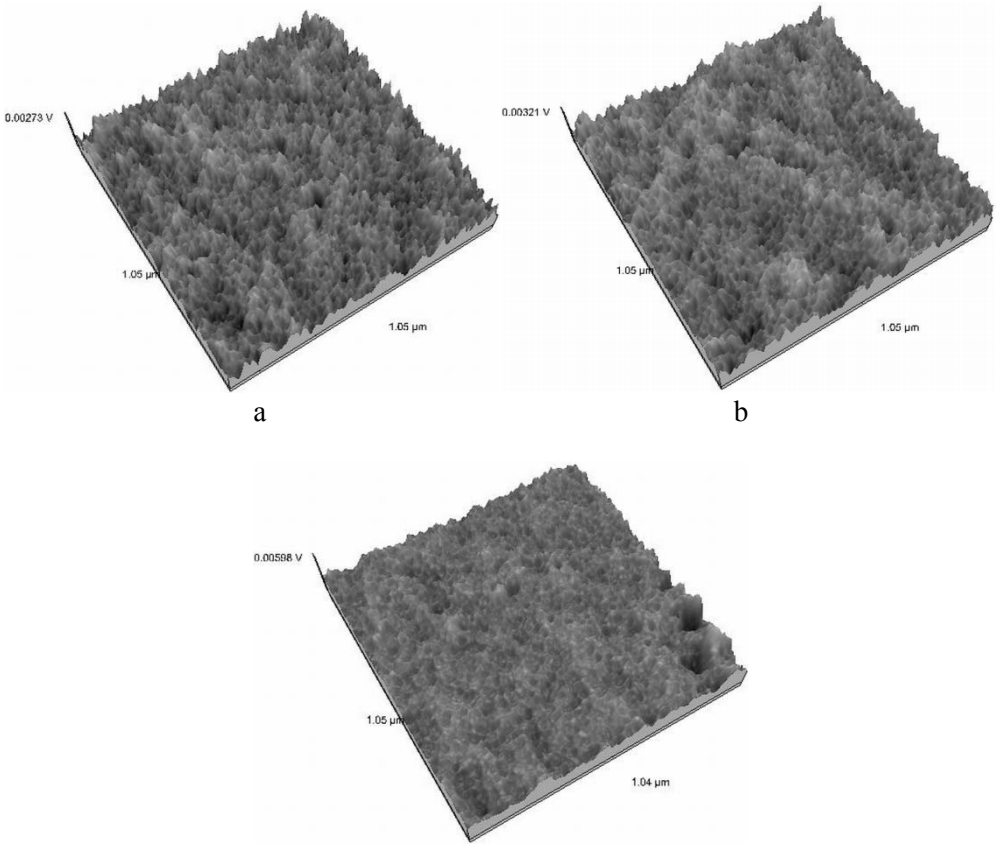

Fig. 4 AFM images of heated $ZnTa_2O_6$ at 1100 °C powders, different pH values. (a) pH=12.5, (b) pH= 10.5, (c) pH= 7

From AFM measurements data, we performed particle size analysis. The average grain size is about ~42 nm for the heated $ZnTa_2O_6$ at 1100 °C, three hours long, when fixing the pH at 12.5; for value of the pH=10.5 is about ~50 nm and grain size for value of the pH=7 is about ~46 nm. The AFM data also show that powders with different mean square root (rms) surface roughness were obtained by varying the value of the pH.

The surface roughness is calculated using the equations [19], for the average roughness is (2):

$$S_a = \frac{1}{MN} \sum_{k=0}^{M-1} \sum_{l=0}^{N-1} \left| z(x_k, y_l) \right| \tag{2}$$

and the mean square root roughness (3):

$$S_{rms} = \sqrt{\frac{1}{MN} \sum_{k=0}^{M-1} \sum_{l=0}^{N-1} \left(z(x_k, y_l) \right)^2} \tag{3}$$

where N and M is the number of crystal axes x and y respectively; z is the average height of crystallites; x_k and y_l are maximum and minimum deviations from the average crystallite.

The values of the heated $ZnTa_2O_6$ at 1100 °C for 3 h for the value pH=12.5 are S_a=0.32 nm and S_q= 0.40 nm; for the value pH=10.5 are S_a=0.27 nm and S_q= 0.36 nm and for the value pH=7 are S_a=0.30 nm and S_q= 0.37 nm, respectively.

The measured data from both SEM and AFM microscopy, revealed an increased value of averige roughness in case of working at the more basic pH 12.5 in comparison with the values of

averige roughness obtained when using pH of the solutions of 10.5 and 7. SEM image (Fig. 3 a) show a multilayer, non-compact disposition of the aggregates generating a large number of small pores. From AFM measurements (Fig.4a) the mean volume of these pores are 5142. By decreasing the pH in basic conditions of synthesis (10.5), a more compacted material has been formed. Instead, by changing the pH conditions to slightly acid (7) the morphology of the surface is more aerated (Fig. 3 c).

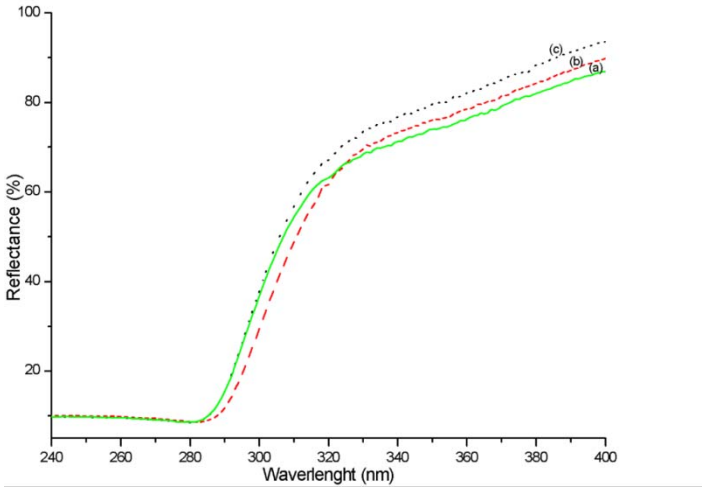

Fig. 5. Diffuse reflectance spectra of heated $ZnTa_2O_6$ at 1100°C: (a) pH=12.5; (b) pH=10.5 and (c) pH=7.
(b)

The diffuse reflectance spectra of the heated $ZnTa_2O_6$ at 1100 °C powders obtained at different the values pH ((a) pH=12.5; (b) pH=10.5 and (c) pH=7) in the UV region are shown in Fig. 5.

The absorbance was calculated from the reflectance using Kubelka–Munk equation [20, 21]. The optical absorption spectra (Fig. 6) of the heated $ZnTa_2O_6$ powders at 1100 °C, obtained at different values of pH ((a) pH=12.5; (b) pH=10.5 and (c) pH=7) are detected in the range of 240-400 nm (or 41666.66-25000 cm^{-1}) at room temperature. From each of the absorption spectra we plotted $\{(k/s)h\nu\}^2$ versus hν (Fig.6), where k denotes absorption coefficient, s is scattering coefficient and hν is the photon energy.

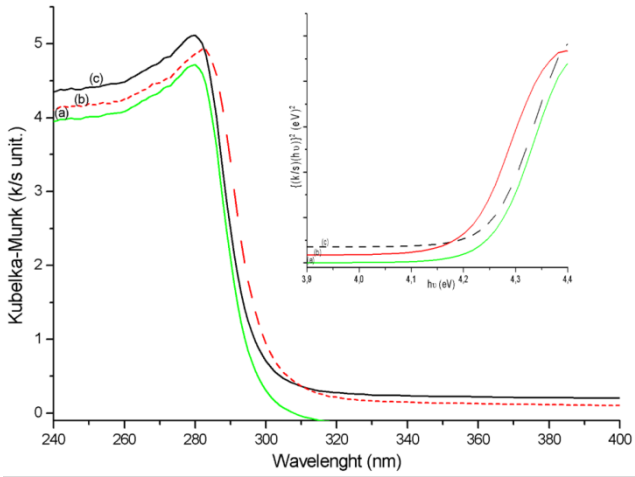

Fig. 6. Absorption spectra of heated ZnTa2O6 at 1100 °C: (a) pH=12.5; (b) pH=10.5 and (c) pH=7. Plot of $\{(k/s)h\nu\}^2$ *vs. hν (energy) of heated* $ZnTa_2O_6$ *at 1100°C: (a) pH=12.5; (b) pH=10.5 and (c) pH=7*

From Fig.6 the band gaps were calculated: 4.30 eV for $ZnTa_2O_6$ at the pH value of 12.5, 4.25 eV for $ZnTa_2O_6$ at the pH value of 10.5 and 4.28 eV for $ZnTa_2O_6$ at the pH value of 7, respectively. The band gaps of the heated $ZnTa_2O_6$ powders at 1100 °C obtained at different values of pH, namely: pH=12.5; pH=10.5 and pH=7 were determined from the absorption spectra.

Therefore, the valence band of $ZnTa_2O_6$ is mainly composed of O 2p orbital hybridized with Zn^{2+} 3d orbital, while orbital of Ta 5d in Ta^{5+} contributes to the formation of conduction band [22].

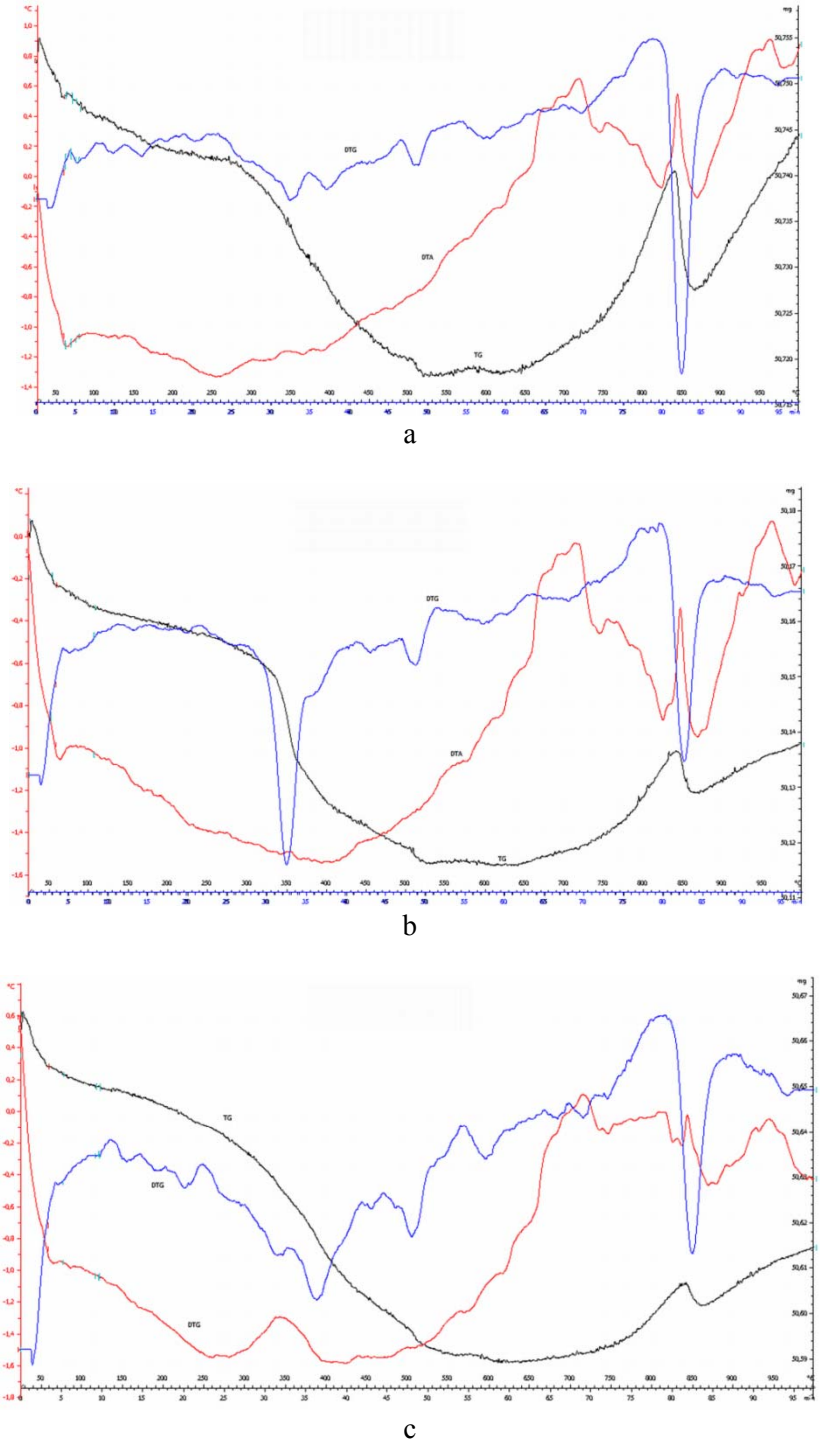

Fig. 7 The DTA, DTG and TG curves of heated $ZnTa_2O_6$ (a) pH=12.5; (b) pH=10.5 and (c) pH=7, heated by a rate of 20 °C/min.

Figs. 7 a, b and c shows the DTA, DTG and TG curves of $ZnTa_2O_6$ (a) pH=12.5; (b) pH=10.5 and (c) pH=7, which were obtained at a heating rate of 20 °C/min.

The main significant feature of the three thermal analysis diagrams (Fig. 7 a, b, c) of the nanomaterials obtained by varying the pH of the media is an important transformation taking place around 850 °C. This transformation has different magnitudes for different obtained materials but display similar characteristics. In the temperatures range of 25-680 °C it can be observed the existence of an endothermic effect that can be attributed to dehydration and dehydroxylation phenomena. Centered at 840 °C, an exothermic effect, associated with a weight increase is observed and might be caused by the oxidation of partial metallic ions. In the domain of 880-1000 °C an exothermic effect is to be noticed that can be assigned to $ZnTa_2O_6$ crystalline network formation [10].

4. Conclusions

$ZnTa_2O_6$ nano-powders were obtained using Ta_2O_5 and $Zn(NO_3)_2$ as the starting materials by solid-state synthesis. A systematic investigation of the structural, morphological, optical, thermal properties of $ZnTa_2O_6$ has been performed by means of various analytical techniques: XRD, FT-IR, SEM, AFM, UV-vis, TGA.

XRD result reveals that the single phase of $ZnTa_2O_6$, can be obtained by heating the nanomaterials at 1100 °C and by fixing different pH conditions of media.

From the FT-IR it is also certified that only sole $ZnTa_2O_6$ phase is present in the sample. The pH value of the environment has not significantly influenced the solid-state process and the size of the obtained particle.

$ZnTa_2O_6$ nanopowders with an average crystallite size of 35 nm, 43 nm and 38 nm can be obtained by heating at 1100 °C the samples at pH=12.5, pH=10.5 and pH=7, respectively. The same dimension of the particles was confirmed by AFM measurements.

The absorption edge of $ZnTa_2O_6$, located at ~283 nm, corresponding to a band gap of in the range 4.25 eV-4.30 eV, very little influenced by the pH conditions, is expected to show excellent performances under UV light irradiation.

The modelling of elementary cell put into evidence that each Zn atom is surrounded by 3 O atoms in a tetrahedral local symmetry (Td), the inter-atomic Zn-O distance being the same and that each Ta atom is surrounded by 5 O atoms in a ortho-rhombic local symmetry.

Acknowledgements

The authors would like to thank to Daniel Ursu, Cornelia Bandas and Paula Sfîrloagă from National Institute for Research and Development in Electrochemistry and Condensed Matter for X-ray diffraction, UV-VIS measurements and SEM measurements. The authors Eugenia Făgădar-Cosma and Corina Enaghe are acknowledging Romanian Academy for financial support in the frame of Programmes 1 and 2 of ICT-AR.

References

[1] Grama S, Hurduc N. Fagadar-Cosma E, Vasile M., Tarabukina E., Fagadar-Cosma G., Digest Journal Of Nanomaterials And Biostructures , **5** (4), 959 (2010).
[2] Enache C., Fagadar-Cosma E., Armeanu I., Dudas Z., Ianasi C. Vasile M., Dascalu D., Digest Journal Of Nanomaterials And Biostructures, **5**(3), 683 (2010).
[3] Vasile M., Vlazan P. and Avram N. M., 2010 J. Alloys Compd., **500** (2) 185
[4] Vasile M., Vlazan P., Sfirloaga P., Grozescu I., Avram N.M. and Rusu, E., Phys. Sc. T, T**135,** 014046 (2009).
[5] Garbarczyk J.E., Wasiucionek M., Jozwiak P., Nowinski J.L. and C.M. Julien, Solid State Ionics, **180** 531 (2009).

[6] Pietrzak T.K., Wewior L., Garbarczyk J.E., Wasiucionek M., Gorzkowska I., Nowinski J.L. and Gierlotka S., Solid State Ionics, **188,** 99 (2011).
[7] Dudas Z., Enache C., Fagadar-Cosma G., Armeanu I. and Fagadar-Cosma E., Mater. Res. Bull. **45** 1150 (2010).
[8] Kong J.Z., Li A.D.,. Zhai H.F,. Gong Y.-P, Li H. and Wu D., J Solid State Chem. **182** 2061 (2009).
[9] Ding Z., Wu W., Liang S., Zheng H. and Wu L., Mat. Lett., **65** 1598 (2011).
[10] Zhang Y.C., Fu B. and Wang X., J. Alloys Compd., **478** 498 (2009).
[11] Lee H.J., Kim I.T. and Hong K.S., Jpn. J. Appl. Phys. **36** 1318 (1997).
[12] Kan A., Ogawa H. and Ohsato H., J. Alloys Compd. **337** 303 (2002).
[13] Huang C.L.,. Chiang K.H, Mater. Res. Bull. **39** 1701 (2004).
[14] Ning P.F., Li L.X., Zhang P., Xia W.S.., 2011 Ceram. Int., doi:10.1016/j.ceramint.2011.09.018
[15] Kunshina G. B., . Bocharova I. V, Gromov O. G., . Lokshin E. P and Kalinnikov V. T., , Inorg. Mat. **48** (1), 62 (2012).
[16] Minami T., Sato H., Ohashi K., Tomofuji T., and Takata S., J. Cryst.Growth **117,** 370 (1992).
[17] Venkatesh J., Subramanian V., Murthy V.R.K, Physica B: Condensed Matter, **293** (1-2), 118 (2000).
[18] Mayer J. M., Inorg. Chem., **27** (22) 3899 (1988).
[19] Kapaklis V., Poulopoulos P., Karoutsos V., Manouras Th., Politis C., Thin Solid Films, **510** 138 (2006).
[20] Kubelka P., Munk F., Zh. Tekh. Fiz. **12** 593 (1931)
[21] Kubelka P., J. Opt. Soc. Am. **38** 448 (1948)
[22] Kudo A., Kato H., Nakagawa S., J Phys Chem B **104** 571 (2000).